

Chemical kinetics of scandium ionization in H₂–O₂–N₂ flames

Jingzhong Guo, John M. Goodings*

Department of Chemistry and Centre for Research in Mass Spectrometry, York University,
4700 Keele Street, Toronto, Ont., Canada M3J 1P3

Received 2 November 2001; accepted 20 December 2001

Abstract

The ionization of scandium was investigated in five premixed, fuel-rich, H₂–O₂–N₂ flames at atmospheric pressure in the temperature range 1820–2400 K. Scandium was introduced ($\leq 10^{-6}$ mol fraction) using an atomizer technique, and the ions were observed by sampling the flame gas through a nozzle into a mass spectrometer. From calculations based on theoretical thermodynamic data, neutral scandium species were present primarily as Sc(OH)₃ with a small amount of OScOH, and the dominant ionic species were Sc(OH)₂⁺ and ScO⁺. This is in good agreement with experimental observations of the ions as members of the oxide ion series ScO⁺·nH₂O ($n = 0–3$). The ionization was observed to receive an initial boost, evidently from the atomic chemi-ionization reaction of Sc with O to form ScO⁺ and free electrons in the flame reaction zone. No other such reaction was calculated to be exothermic. Thermal (collisional) ionization of ScO is negligible. When a trace of methane was added to produce H₃O⁺ as a chemical ionization (CI) source, scandium ions were formed by proton transfer with a global rate constant given by $k_{PT} = (9.58 \pm 0.76) \times 10^{-23} T^{3.92 \pm 0.62} \text{ cm}^3 \text{ molecule}^{-1} \text{ s}^{-1}$; it exhibits a positive temperature dependence with an activation energy barrier of 16.2 kcal mol⁻¹. The global recombination coefficient for scandium ions with electrons is given by $k_{Sc} = (3.72 \pm 0.22) \times 10^{-4} T^{-1.03 \pm 0.26} \text{ cm}^3 \text{ molecule}^{-1} \text{ s}^{-1}$ with the expected negative temperature dependence. (Int J Mass Spectrom 214 (2002) 349–364) © 2002 Elsevier Science B.V. All rights reserved.

Keywords: Scandium; Flame ionization; Gas phase; Chemical kinetics; Mass spectrometry

1. Introduction

Since 1988, we have been interested in the flame ionization of group 3 metals and lanthanide metals [1–7]. In 1995, we reported a qualitative study of the group 3 (or 3B) metals La, Y and Sc in H₂–O₂–Ar flames [2]; the positive ions observed could be represented by the members of an oxide ion series AO⁺·nH₂O ($n = 0–3$), where A is the metal atom. The study was extended to include the further lanthanide metals Ce, Pr, and Nd [3]. Later, quantitative studies of the chemical kinetics of Y [6] and La [7]

were carried out in well-characterized H₂–O₂–N₂ flames. These metals exist in flames as a variety of neutral species, some of which have relatively low ionization energies (e.g., odd electron species such as AO), very strong A=O bonds and high proton affinities. All of these factors are involved in the flame ionization of these metals.

Very recently, we completed density functional studies on ScH_xO_y neutrals and ions [8,9]. These calculations have provided more accurate structural and energetic information than is available for the other metals. Therefore, the information for scandium is more definitive in ascertaining the relative importance of different ionization mechanisms in flames which

* Corresponding author. E-mail: goodings@yorku.ca

include chemical ionization (CI) by H_3O^+ , thermal (collisional) ionization and chemi-ionization. With knowledge of the ionization mechanisms, a major objective has been quantitative measurements of the chemical kinetics for production and loss of scandium ions, i.e., values of rate coefficients and their temperature dependencies.

2. Computational methods

In our previous theoretical studies of Sc species, energies, equilibrium structures and vibrational frequencies were obtained using density functional methods with the Gaussian 98 suite of programs. Details and evaluations of the ab initio calculations with density functional methods have already been given [8,9]. With energies from the B3LYP/6-311++G(3df,3pd) method as well as structures and vibrational frequencies from the BP86/6-311++G(3df,3pd) method, thermodynamic data for all Sc species can be derived at flame temperatures using the standard techniques of statistical mechanics [10]. Thus, the equilibrium compositions of the five flames employed when doped with Sc are well known, both with respect to Sc species from our calculated data and for other species using values from the JANAF Tables [11].

3. Experimental

Five well-characterized $\text{H}_2\text{-O}_2\text{-N}_2$ flames in the temperature range 1820–2400 K were employed for this work, and their properties are specified in Table 1. Each is a premixed, flat, laminar flame of fuel-rich composition burning at atmospheric pressure with the burnt gas downstream of the reaction zone in plug flow at essentially constant velocity, providing a time axis for chemical kinetics. The concentrations of the free radicals H, OH and O overshoot their equilibrium values in the flame reaction zone and then decay downstream towards equilibrium in the burnt gas; the effect is greater, the cooler the flame. The degree of overshoot is specified by Sugden's disequilibrium parameter γ [12] defined as the ratio of the actual concentration of a species at any point in the flame to its equilibrium concentration at the flame temperature T . For fuel-rich flames where $[\text{H}_2\text{O}]$ and $[\text{H}_2]$ are constant throughout the burnt gas, $\gamma_{\text{H}} = \gamma_{\text{OH}} \equiv \gamma$ whereas $\gamma_{\text{O}} = \gamma^2$. For the five flames employed here, Butler and Hayhurst [13] have measured γ as a function of the distance z along the flame axis, i.e., the radical concentrations are known at all points in the flames. Even at $z = 30$ mm downstream in flames 3, 4, 5, $\gamma \neq 1$. All five fuel-rich flames are cylindrical in shape with a diameter of about 12 mm. These

Table 1
Properties of the hydrogen–oxygen–nitrogen flames

Property	Flame 2	Flame 25	Flame 3	Flame 4	Flame 5
Equivalence ratio, ϕ	1.37	1.5	1.59	1.55	1.5
$\text{H}_2/\text{O}_2/\text{N}_2$	2.74/1/2.95	3.0/1/3.5	3.18/1/4.07	3.09/1/4.74	3.0/1/3.55
Total unburnt gas flow (mL s^{-1})	300	250	250	200	150
Measured flame temperature T_f (K)	2400	2230	2080	1980	1820
Rise velocity in burnt gas v_f (m s^{-1})	19.8	16.2	15.6	11.4	8.4
Cross-sectional area A ($\times 10^{-4} \text{ m}^2$)	1.05	1.01	0.993	1.04	0.990
Equilibrium burnt gas composition (mol fractions)					
H_2O	0.3460	0.3063	0.2754	0.2553	0.2249
H_2	0.1286	0.1527	0.1622	0.1390	0.1259
O_2	0.0001057	0.00000790	0.00000072	0.00000018	0.00000001
H	0.006019	0.002650	0.001077	0.0005008	0.0001415
OH	0.003084	0.0007951	0.0002130	0.00008890	0.00001754
O	0.00009469	0.00000935	0.00000099	0.00000023	0.00000001
N_2	0.5157	0.5375	0.5610	0.6052	0.6490

pseudo-one-dimensional (flat) flames were stabilized on a water-cooled brass burner previously described [4], consisting basically of a circular bundle of 151 stainless steel hypodermic tubes.

Scandium was introduced into the flames by spraying an aqueous solution of ScCl_3 (Aldrich, 99.99% pure) into the premixed flame gas as an aerosol derived from a pneumatic atomizer [14]; it is operated by a flow of 16.2 mL s^{-1} of the diluent nitrogen gas. Spraying a 0.1 M solution introduced approximately 1×10^{-6} mol fraction of total scandium into a premixed flow of 250 mL s^{-1} . In this study, two aqueous solutions of 0.02 and 0.1 M ScCl_3 were employed. The scandium-doped flames were fuchsia in color. After the flame had been burning for a few minutes, a white solid (presumably oxide) condensed onto the cold sampling plate in a pattern of multiple distorted hexagons, each little hexagon being associated with one hypodermic burner tube. The five $\text{H}_2\text{-O}_2\text{-N}_2$ flames used in the present work exhibit only a very low level of natural ionization. For some kinetics measurements, a constant flow rate of 0.415 mL s^{-1} of CH_4 was added to the premixed gas in order to produce a high initial concentration of H_3O^+ ions in the flames by chemi-ionization. For the five flames 2, 25, 3, 4 and 5 listed in Table 1, this amounts to 0.14, 0.17, 0.17, 0.21 and 0.28 mol% of the unburnt gas, respectively.

The burner was mounted horizontally on a motorized carriage with calibrated drive, and the flame axis was accurately aligned with the sampling nozzle of the mass spectrometer. The apparatus has been described in detail previously [4], so only a brief description will be given here. Flame gas containing ions is sampled through an orifice $\sim 0.16 \text{ mm}$ in diameter in the tip of a conical nozzle protruding from a water-cooled sampling plate of stainless steel. Both blunt nozzles which make use of a Pt/Ir electron microscope lens and sharp nozzles of electroformed Cr were employed [4]. The ions enter a first vacuum chamber maintained at $\sim 0.04 \text{ Pa}$ (3×10^{-4} Torr), are focused into a beam by an electrostatic lens and pass through a 3 mm orifice in a nose cone into a second vacuum chamber maintained below 0.003 Pa ($< 2 \times 10^{-5}$ Torr). The ions are focused

again by a second ion lens for analysis by a quadrupole mass filter, collected by a parallel-plate Faraday detector and measured by a sensitive electrometer connected to the *Y*-axis of an *XY*-recorder. Measured ion signal magnitudes in the figures are given in millivolts (mV); they refer to the collected ion current passing through a grid-leak resistor of $10^{10} \Omega$. By driving a flame toward the sampling nozzle, the profile of an individual ion signal vs. distance z along the flame axis can be obtained; the distance z is coupled to the *X*-axis of the *XY*-recorder. The designation of $z = 0$ is arbitrarily taken as a fixed distance ($\sim 6 \text{ mm}$) between the burner face and the sampling plate. In practice, this means that the nozzle tip is located just downstream of the luminous reaction zone when $z = 0$.

As an alternative to individual ions, total positive ion (TPI) profiles can be measured by switching off the dc voltages to the quadrupole rods. Still, with the dc voltages switched off and the spectrometer's mass dial set to a given mass number, all of the ions above that mass number are collected. For example, TPI_{50} designates total positive ions above 50 u, whereas TPI_{12} includes all of the ions because no flame ions exist below 12 u. This technique is useful in separating total scandium ions from ions of low mass number such as H_3O^+ , Na^+ and K^+ , if present. However, the sensitivity of the mass spectrometer is different for individual ions which are measured at fairly high resolution and TPI collection which amounts to zero resolution. The former sensitivity is approximately one-half of the latter. Negative ions were never detected in the five flames doped with Sc. This means that [TPI] is always equal to the total concentration of free electrons [e^-] because a flame is a quasi-neutral plasma. When the gas is sampled through the nozzle, it cools in two regions: in the thermal boundary layer surrounding the orifice, and in the near-adiabatic expansion downstream of the nozzle throat. This can cause a shift of fast equilibrium reactions in the exothermic direction during sampling. In particular, ion hydrates can be enhanced with respect to the parent ion. These sampling problems have been discussed in considerable detail [15–17]. They are obviated in the present study by measuring TPI_{50} such that hydrate

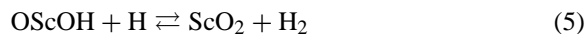
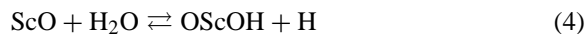
contributions are included in the parent scandium ion signals.

A novel, simple and accurate technique which we now use frequently involves total cation collection at the front nozzle plate [18,19]. When it is biased negatively (~ -50 V) with respect to the burner, free electrons are stopped from reaching the nozzle plate which collects only the total cation current given by $i_+(\text{N}) = eAn_+(\text{N})v_f$, where e is the electron charge, A the flame's cross-sectional area, $n_+(\text{N})$ is the cation density at the nozzle and v_f is the rise velocity in the burnt gas (see Table 1). Since $i_+(\text{N})$ can be readily measured with a picoammeter, $n_+(\text{N})$ can be easily and accurately determined in the five well-characterized flames employed for this study. It is then a simple matter to calibrate the sensitivity of the mass spectrometer. The expression is also employed to calibrate the atomizer delivery by spraying a weak aqueous solution ($<10^{-4}$ M) of CsCl, because Cs is completely ionized in the burnt gas of a hot flame under these conditions.

4. Results and discussion

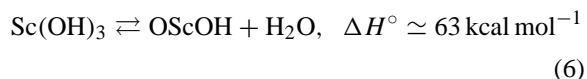
4.1. Neutral scandium species in flames

When aqueous ScCl_3 solution is sprayed into the flames, the aerosol droplets from the atomizer evaporate in the connecting tube containing dry pre-mixed flame gas and enter the burner as crystallites of $\text{ScCl}_3 \cdot n\text{H}_2\text{O}$. The crystallites dissociate in the flame's preheat zone and early reaction zone to produce atomic Sc initially. A subsequent series of fast bimolecular reactions results in a variety of scandium species which might include the 11 neutrals Sc, ScH, ScO, ScOH, HScO, ScO_2 , HScOH, OScOH, Sc(OH)_2 , HSc(OH)₂ and Sc(OH)_3 . After the O_2 oxidant is exhausted in the reaction zone, the major species in these fuel-rich flames are H_2O , H_2 , H and OH (see Table 1). Ten bimolecular reactions can be written, each for a pair of Sc neutrals, such as:



From calculated structures, vibrational frequencies and energies for the 11 Sc neutrals [8], thermodynamic values, specifically $\Delta_f G_T^\circ$, were calculated at each of the five flame temperatures given in Table 1 using the standard methods of statistical mechanics. With similar data for H_2O , H and OH from the JANAF Tables [11], equilibrium constants K for the 10 bimolecular reactions were then calculated to give 10 concentration ratios of the 11 Sc neutrals in terms of K , $[\text{H}_2\text{O}]$, $[\text{H}_2]$, $[\text{H}]$ and $[\text{OH}]$. The mole fractions of the latter flame neutrals are given in Table 1 for all five flames. It is then an easy matter to determine the percentage of each Sc neutral at equilibrium in each of the five flames. The procedure has been described previously in more detail, specifically for flame 2 [10].

The calculations show that just four Sc neutral species (Sc(OH)_3 , OScOH, ScO and Sc(OH)_2 , in decreasing order) are dominant, totaling >99.8% of the total scandium in each flame; the other species are negligible. The results are given as fractions in Table 2, and the behavior of the major species is illustrated in Fig. 1 to show the trends with flame temperature T at a glance. The trihydroxide Sc(OH)_3 is by far the dominant neutral, even more so as T decreases from 2400 (flame 2) to 1820 K (flame 5). In flame 2, OScOH, ScO, and Sc(OH)_2 are also appreciable but all three species decrease rapidly as T decreases. These results, particularly for Sc(OH)_3 and OScOH, are probably not surprising because neutral Sc as a group 3 metal prefers the +3 oxidation state. Also, the high $[\text{Sc(OH)}_3]/[\text{OScOH}]$ ratio is expected because water is such a major product in the burnt gas of these flames



where ΔH_6° is always endothermic. Although nearly 20% of Sc(OH)_3 breaks down to form OScOH in the hottest flame 2, the value of the equilibrium constant

Table 2
Calculated fractions of neutral scandium species in the five flames

Neutral species	Flame 2	Flame 25	Flame 3	Flame 4	Flame 5
Sc	2.618E-7	5.249E-8	7.198E-9	1.180E-9	6.076E-11
ScO	2.116E-2	6.174E-3	1.415E-3	4.180E-4	5.319E-5
ScH	2.423E-9	5.976E-10	9.666E-11	1.604E-11	8.763E-13
ScOH	1.656E-5	5.760E-6	1.506E-6	4.407E-7	5.790E-8
HScO	2.307E-4	8.423E-5	2.317E-5	7.051E-6	9.975E-7
HScOH	4.710E-6	2.214E-6	7.548E-7	2.418E-7	3.915E-8
ScO ₂	9.606E-4	1.305E-4	1.633E-5	3.759E-6	2.561E-7
OScOH	1.734E-1	7.656E-2	2.924E-2	1.398E-2	3.816E-3
Sc(OH) ₂	8.091E-3	5.087E-3	2.670E-3	1.452E-3	5.231E-4
HSc(OH) ₂	4.907E-4	4.444E-4	3.240E-4	2.028E-4	9.971E-5
Sc(OH) ₃	7.956E-1	9.115E-1	9.663E-1	9.839E-1	9.955E-1
Total	1.0000	1.0000	1.0000	1.0000	1.0000

K_6 decreases with decreasing T such that correspondingly less OScOH is formed. It does not follow that every Sc (+3) species will be abundant; e.g., the H–Sc bond in HSc(OH)₂ is relatively weak [10]. The less stable ScO and Sc(OH)₂ are more minor neutral species in the +2 oxidation state with one odd electron. The other scandium neutrals are considerably less abundant as shown in Table 2.

4.2. Ionic scandium species in flames

Using the methods and data from our previous studies [8–10], the energies, structures, vibrational frequencies and thermodynamic properties were calculated for 20 scandium ions ScH_xO_y⁺. In exactly the same way as described in the Section 4.1 for the 11 scandium neutrals, the fractions of the 20 ions at

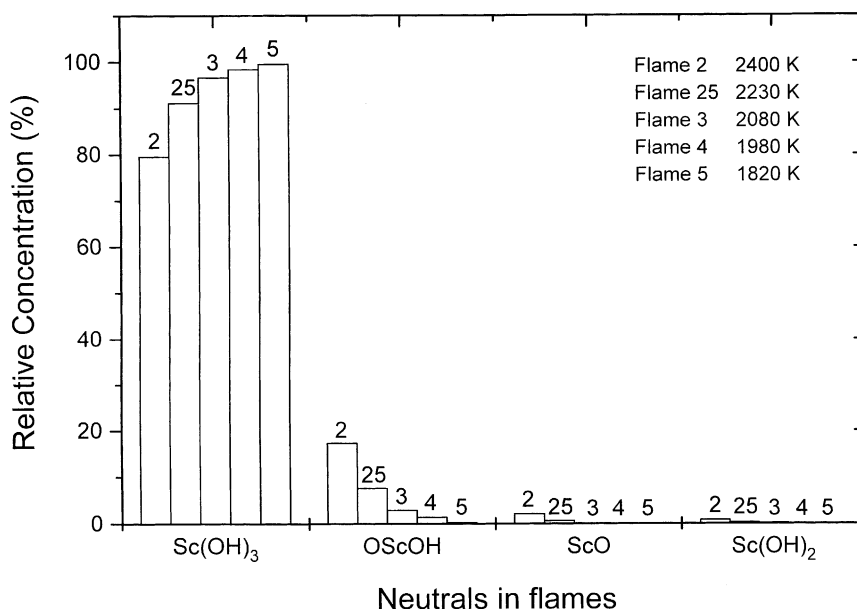
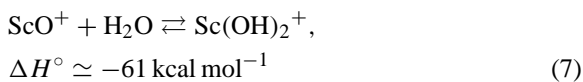


Fig. 1. Major scandium neutral species in the five flames calculated at thermal equilibrium.

Table 3
Calculated fractions of scandium ions in the five flames

Ionic species	Flame 2	Flame 25	Flame 3	Flame 4	Flame 5
Sc ⁺	5.721E-5	2.582E-5	7.971E-6	2.457E-6	3.232E-7
ScO ⁺	5.778E-1	3.554E-1	1.714E-1	9.053E-2	2.685E-2
ScH ⁺	1.061E-6	6.014E-7	2.230E-7	7.071E-8	1.028E-8
ScOH ⁺	1.158E-2	9.628E-3	6.034E-3	3.485E-3	1.283E-3
HScO ⁺	8.844E-7	2.673E-7	5.986E-8	1.602E-8	1.441E-9
Sc ⁺ ·H ₂ O	5.069E-7	3.693E-7	1.931E-7	8.727E-8	2.156E-8
HScOH ⁺	7.541E-5	7.747E-5	5.758E-5	3.392E-5	1.364E-5
ScO ₂ ⁺	2.105E-6	3.574E-7	5.309E-8	1.423E-8	1.031E-9
OScOH ⁺	6.745E-4	2.681E-4	9.070E-5	4.047E-5	7.850E-6
Sc(OH) ₂ ⁺	4.051E-1	6.264E-1	8.076E-1	8.841E-1	9.321E-1
ScOH ⁺ ·H ₂ O	9.434E-5	1.182E-4	1.177E-4	9.530E-5	6.100E-5
HSc(OH) ₂ ⁺	1.207E-7	8.935E-8	5.221E-8	2.830E-8	8.697E-9
Sc ⁺ ·2H ₂ O	1.716E-9	1.549E-9	1.116E-9	6.634E-10	2.456E-10
Sc(OH) ₃ ⁺	2.084E-5	1.441E-5	8.984E-6	6.294E-6	2.621E-6
Sc(OH) ₂ ⁺ ·H ₂ O	2.641E-3	6.272E-3	1.313E-2	2.051E-2	3.895E-2
ScOH ⁺ ·2H ₂ O	4.645E-7	8.124E-7	1.191E-6	1.279E-6	1.290E-6
Sc(OH) ₂ ⁺ ·2H ₂ O	7.305E-7	2.451E-6	7.641E-6	1.597E-5	4.861E-5
ScO ⁺ ·H ₂ O	1.907E-3	1.861E-3	1.502E-3	1.156E-3	6.403E-4
ScO ⁺ ·2H ₂ O	2.332E-6	3.256E-6	3.968E-6	4.128E-6	3.729E-6
ScO ⁺ ·3H ₂ O	2.368E-10	5.165E-10	7.971E-10	1.032E-9	1.383E-9
Total	1.0000	1.0000	1.0000	1.0000	1.0000

thermal equilibrium calculated at each of the five flame temperatures are given in Table 3. All 20 ions are accounted for by Sc⁺, ScO⁺, ScOH⁺, Sc(OH)₂⁺ and their hydrates. However, the calculations show that just four ions (Sc(OH)₂⁺, ScO⁺, Sc(OH)₂⁺·H₂O and ScOH⁺, in decreasing order) amount to >99.7% of the total, as shown in Fig. 2. Of the two dominant ions in all five flames, Sc(OH)₂⁺ increases with decreasing *T* while ScO⁺ decreases rapidly. This implies that these two ions are linked by a hydration–dehydration equilibrium:



for which ΔH° is always exothermic in the forward direction. As *T* decreases for the equilibrium reaction, Sc(OH)₂⁺ is favored. Not surprisingly, the behavior of the minor monohydrate Sc(OH)₂⁺·H₂O mimics that of its parent ion. The other still more minor species ScOH⁺ decreases as *T* decreases.

These calculated values can be compared with the scandium ions and their relative concentrations actu-

ally observed in the flames as shown in Fig. 3 with the atomizer spraying a 0.02 M solution of ScCl₃. The five flames were also doped with 0.415 mL s⁻¹ of CH₄ (0.14–0.28 mol% for flames 2–5, respectively) and sampled downstream at *z* = 30 mm using a Pt/Ir nozzle of orifice diameter 0.160 mm. Scandium ions were observed at mass numbers *M* 61, 79, 97, 115 and 133 u, and can be represented by a hydrate series ScO⁺·*n*H₂O (*n* = 0–4). Although 61 can only be ScO⁺, isomers are possible at the other mass numbers: ScO⁺·H₂O or Sc(OH)₂⁺ at 79; ScO⁺·2H₂O or Sc(OH)₂⁺·H₂O at 97; ScO⁺·3H₂O or Sc(OH)₂⁺·2H₂O at 115; and ScO⁺·4H₂O or Sc(OH)₂⁺·3H₂O at 133. With decreasing *T*, more and more ions were detected as hydrates as seen in Fig. 3. In additional experiments, fewer hydrates were observed when a bigger orifice was employed, showing that hydrates are formed due to cooling during sampling. At first glance, the experimental results in Fig. 3 might appear to be quite different from the theoretical ones in Fig. 2; in fact, the agreement is very good. Our calculations indicated

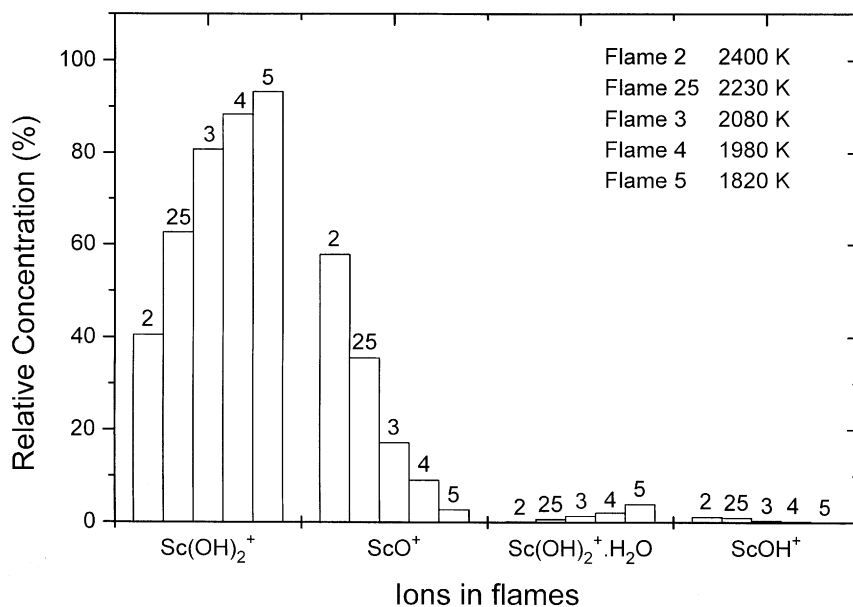


Fig. 2. Major scandium ionic species in the five flames calculated at thermal equilibrium.

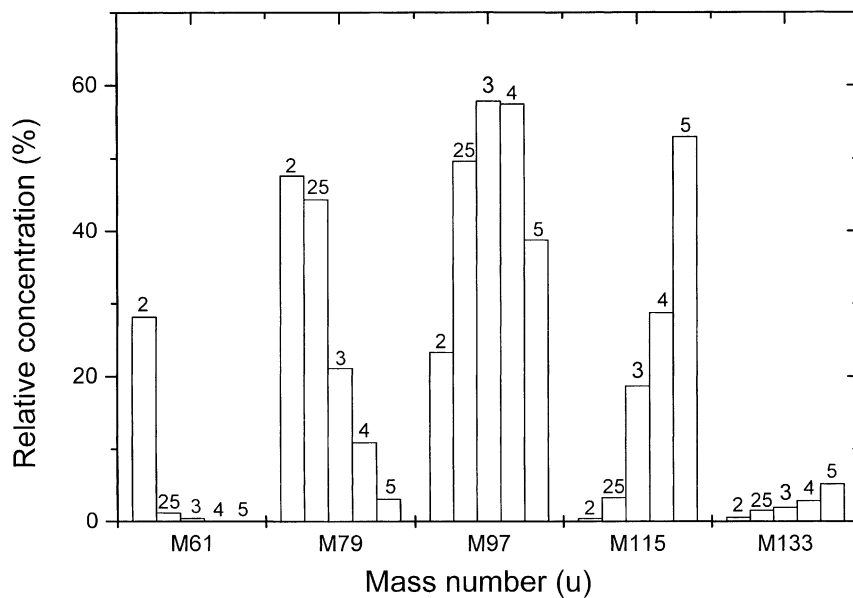


Fig. 3. Scandium ionic species observed in the five flames with the atomizer spraying a 0.02M solution of ScCl₃. The flames were doped with a small amount of CH₄ and were sampled downstream at $z = 30$ mm with a Pt/Ir nozzle of orifice diameter 0.160 mm.

that essentially only two ions (ScO^+ and $\text{Sc}(\text{OH})_2^+$) of the 20 considered have a genuine existence in flames, and these two ions were observed experimentally. As expected, theoretical calculations showed that all scandium ions have hydration energies which are exothermic [9]. This means that hydrates are predicted to form readily by the cooling which occurs during sampling. Thus, although more hydrate ions were detected experimentally by the mass spectrometer, the hydrates are not genuine flame ions.

4.3. Production of scandium ions in flames

The possible processes for the production of scandium ions in flames are (a) chem-ionization; (b) CI; and (c) thermal (collisional) ionization. Based on our calculations of $\Delta_f H^\circ$ for scandium species and values from the JANAF Tables [11], it was determined previously [10] that the only exothermic chemi-ionization

reaction is



because $D^\circ(\text{Sc-O})$ exceeds $\text{IE}^\circ(\text{ScO})$. Other such reactions involving the major flame neutrals $\text{Sc}(\text{OH})_3$ and OScOH reacting with H to give $\text{ScO}^+ \cdot n\text{H}_2\text{O}$ ions are just too endothermic to be feasible [10]. The problem arises that both $[\text{Sc}]$ and $[\text{O}]$ are very small at thermal equilibrium (see Tables 1 and 2). However, reaction (8) can provide an initial boost to the ionization of scandium as shown in the profile given in Fig. 4 because of the conditions which prevail during a very short time interval in the flame reaction zone.

An estimate can be made of the ionization level $R_8 \times \delta t$ which can be achieved, where $R_8 = k_8[\text{Sc}][\text{O}]$ is the reaction rate and $\delta t = 1 \mu\text{s}$ is the time interval corresponding to a distance δz of 0.02 mm in flame 2 at 2400 K. A value for $k_8 = 3.4 \times 10^{-14} \text{ cm}^3 \text{ molecule}^{-1} \text{ s}^{-1}$ is taken from the rate coefficient for the chemi-ionization of $\text{Ca} + \text{OH}$

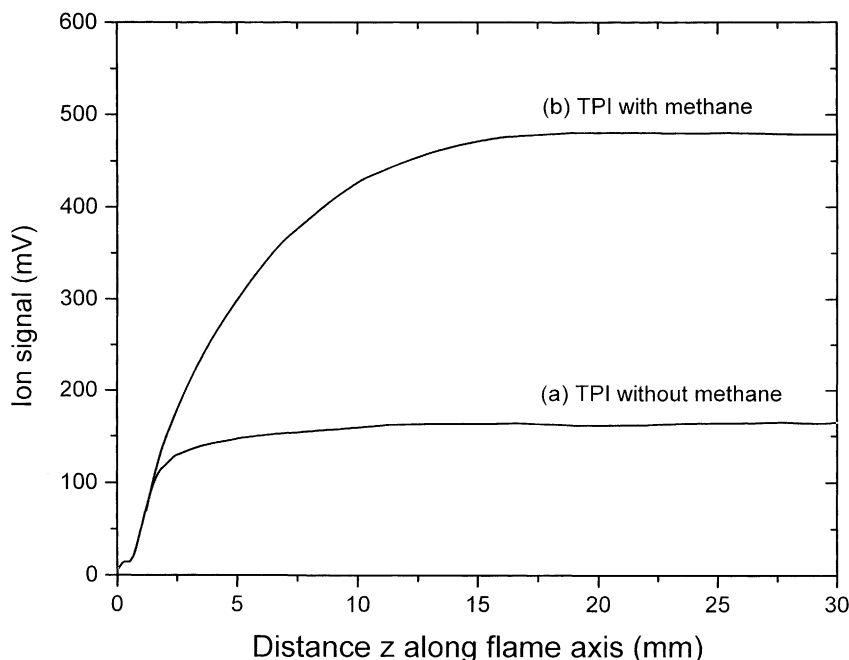
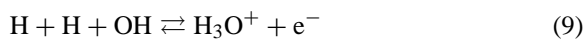


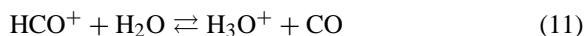
Fig. 4. Mass spectrometric profiles of the total positive ion signal in flame 2 with the atomizer spraying a $\sim 0.1 \text{ M}$ solution of ScCl_3 (a) without CH_4 additive, and (b) when the flame was additionally doped with $\sim 0.093 \text{ mol\%}$ CH_4 . A sharp Cr nozzle of orifice diameter 0.162 mm was employed.

(or $\text{CaO} + \text{H}$) to give CaOH^+ and e^- at 2400 K [20]; Ca is just 1 atomic number lower than Sc. Scandium enters the flame as crystallites of ScCl_3 which dissociate in the preheat zone and early reaction zone to give Sc atoms initially before oxidation to oxides and hydroxides occurs. Suppose that all of the scandium is present as atomic Sc in the narrow time interval of 1 μs . This gives $[\text{Sc}] = 3 \times 10^{12} \text{ atoms cm}^{-3}$ with the atomizer spraying a 0.1 M solution of ScCl_3 as in Fig. 4. Using a rather conservative value of $\gamma = 10$ for the radical overshoot in flame 2 [13], $[\text{O}] = 3 \times 10^{16} \text{ atoms cm}^{-3}$; the high value arises because $[\text{O}]$ varies as γ^2 times the equilibrium concentration given in Table 1. Multiplied together, these numbers yield an ion concentration $[\text{ScO}^+] = 3 \times 10^9 \text{ ions cm}^{-3}$ produced in the short time interval in the flame reaction zone. This is slightly greater than the concentration of $\sim 2 \times 10^9 \text{ ions cm}^{-3}$ observed with the mass spectrometer corresponding to the plateau value of $\sim 150 \text{ mV}$ in Fig. 4. Perhaps not all of the scandium is present as Sc atoms in the time interval $\delta t = 1 \mu\text{s}$. However, the estimate does indicate that reaction (8) can account for the initial boost of scandium ionization observed with the mass spectrometer. A more accurate determination would be extremely difficult.

It is well known that H_3O^+ always exists in undoped $\text{H}_2\text{-O}_2\text{-N}_2$ flames to some degree [21], produced by chemi-ionization:

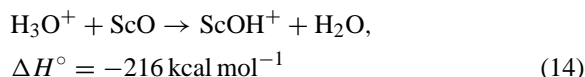
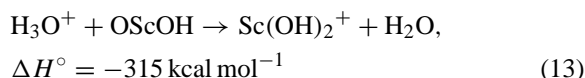
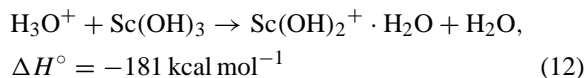


probably involving a two-step mechanism with excited H_2O^* or H_2^* as an intermediate [22]. When even a trace of a hydrocarbon is introduced, a large amount of H_3O^+ is formed near the luminous reaction zone of flames by the well-known sequence [23]:



such that H_3O^+ is the dominant ion throughout the burnt gas region. Thus, it is obviously necessary to consider CI reactions involving H_3O^+ in flames doped with scandium. Our theoretical studies showed that the proton affinities for all scandium neutral species

($>200 \text{ kcal mol}^{-1}$ [9]) are much higher than that of H_2O ($165.2 \text{ kcal mol}^{-1}$ [24]) such that proton transfer will invariably be exothermic, e.g.,



These ΔH° values all refer to 2000 K, but they change little with temperature in the range 1820–2400 K for the five flames in Table 1. Thus, many scandium ions including those from the dominant scandium neutrals can be formed easily by proton transfer with H_3O^+ in flames. This is shown by the upper curve in Fig. 4 when 0.093 mol% of CH_4 was added to flame 2 already doped with scandium.

Thermal (collisional) ionization is another possible source to produce ions in flames because group 3 metals have one easily ionizable odd electron after forming the monoxide with a very strong $\text{A}=\text{O}$ bond. We have demonstrated previously that thermal ionization can be a major mechanism in the case of LaO where the ionization energy is low (4.90 eV) [7], and even to a small extent for YO (5.85 eV) [6]. The ionization energies of the major scandium neutrals which exist in flames are 10.1 eV for $\text{Sc}(\text{OH})_3$, 9.5 eV for OScOH , 6.6 eV for ScO and 6.2 eV for $\text{Sc}(\text{OH})_2$ compared with 6.561 eV for Sc [8]. Thermal ionization for most of these scandium neutrals is too endothermic to warrant serious consideration, particularly for the two dominant species $\text{Sc}(\text{OH})_3$ and OScOH with Sc in the +3 oxidation state. Even for the minor neutrals ScO and $\text{Sc}(\text{OH})_2$ with an easily ionizable odd electron, the ionization energies are much higher than that for LaO and higher than that for YO . Thus, even in higher temperature flames with ScO and $\text{Sc}(\text{OH})_2$ present in small but appreciable concentrations, thermal ionization will not make a measurable contribution to the formation of scandium ions.

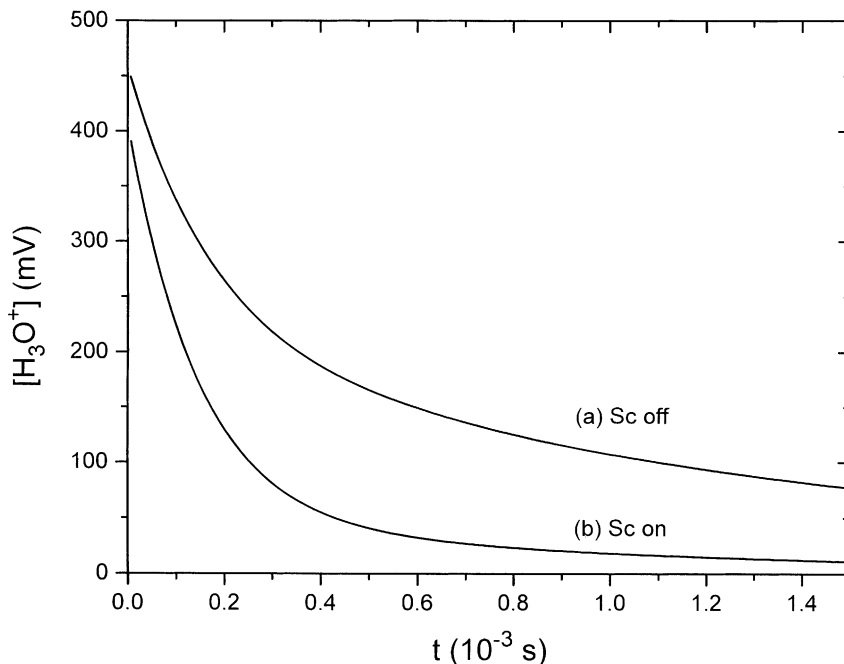
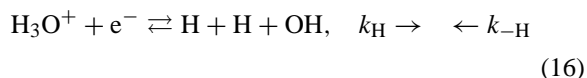
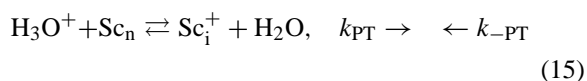


Fig. 5. Mass spectrometric profiles of H_3O^+ in flame 2 doped with 0.14 mol% CH_4 (a) without scandium, and (b) with the atomizer spraying a 0.1 M solution of ScCl_3 . A Pt/Ir nozzle of orifice diameter 0.160 mm was employed.

4.4. Global kinetics of proton transfer to scandium species

Proton transfer to scandium neutrals by H_3O^+ was further confirmed by experimental measurements of H_3O^+ profiles as showed in Fig. 5. When ~ 0.28 mol% of CH_4 was added to flame 2, a high concentration of H_3O^+ was formed in the flame reaction zone. The upper profile shows the recombination loss of H_3O^+ with e^- when the scandium atomizer was turned off. With scandium turned on, the lower profile shows a big drop of $[\text{H}_3\text{O}^+]$, caused by proton transfer to scandium neutrals. It is not possible to do kinetics measurements for individual scandium ions because the relative magnitudes of the ion profiles are altered by cooling during sampling. Nevertheless, global kinetics can be done because the total neutral concentration is well known from calibration of the atomizer delivery; the cooling effect during sampling does not change the total ion concentration.

For the analysis of the proton transfer kinetics, two reactions in both forward and backward directions need to be considered:



where Sc_n represents all scandium neutral species and Sc_n^+ represents all scandium ions. The rate coefficients k for proton transfer (15) and for H_3O^+ recombination/formation (16) are designated beside the reactions. Based on this mechanism, a kinetic expression for the net loss of H_3O^+ can be derived:

$$\begin{aligned} -\frac{d \ln[\text{H}_3\text{O}^+]}{dt} &= k_{\text{H}}[\text{e}^-] + \frac{k_{-\text{H}}[\text{H}][\text{H}][\text{OH}]}{[\text{H}_3\text{O}^+]} \\ &= k_{\text{PT}}[\text{Sc}_n] - \frac{k_{-\text{PT}}[\text{H}_2\text{O}][\text{Sc}_n^+]}{[\text{H}_3\text{O}^+]} \end{aligned} \quad (17)$$

Experimentally, the ion profiles for H_3O^+ , TPI and total scandium ions (TSI) were measured with the mass spectrometer. The conversion of these ion profiles along the flame axis measured as a mass spectrometric signal (mV) to absolute ion concentrations was calibrated by the total cation collection method outlined in Section 3 [18,19]. All neutral concentrations are known because the five flames are well characterized (see Table 1) and $[\text{Sc}_n]$ is given by the atomizer calibration factor. Also, k_{H} [19] and $k_{-\text{H}}$ [25] are known from previous measurements. The logarithmic derivative was obtained from accurate curve fitting of the profiles by a known mathematical function. Plots of the left-hand side of Eq. (17) against $[\text{H}_2\text{O}][\text{Sc}_i^+]/[\text{H}_3\text{O}^+]$ gave good straight lines whose slopes and intercepts yield the rate constants $k_{-\text{PT}}$ and k_{PT} , respectively. It was interesting to note that, although reaction (16) makes a relatively small contribution, the linearity of the plots was greatly improved by its inclusion. Fig. 6 shows a sample plot from measurements for flame 2 doped with 0.14 mol%

CH_4 and 0.02 M ScCl_3 solution. This plot gives a forward global $k_{\text{PT}} = 1.82 \times 10^{-9} \text{ cm}^3 \text{ molecule}^{-1} \text{ s}^{-1}$ at 2400 K. In contrast, the backward $k_{-\text{PT}} = 3.87 \times 10^{-16} \text{ cm}^3 \text{ molecule}^{-1} \text{ s}^{-1}$ is much smaller, consistent with the large endothermicity of the reverse proton transfer reaction.

In the same way, proton transfer coefficients were measured in the five flames at different temperatures from 1820 to 2400 K. The temperature dependence of k_{PT} is shown in Fig. 7. A reasonably good straight line though the logarithmic plot yields $k_{\text{PT}} = (9.58 \pm 0.76) \times 10^{-23} T^{3.92 \pm 0.62} \text{ cm}^3 \text{ molecule}^{-1} \text{ s}^{-1}$ with a positive temperature dependence. Normally, proton transfer reactions are expected to have a negative temperature dependence. Our different result can be explained by the complication of measuring a global proton transfer reaction. Global proton transfer includes more than one primary reaction, and several steps may be involved. Some steps, say dehydration or isomerization of ionic hydrates produced in primary reactions, may be endothermic. The Arrhenius

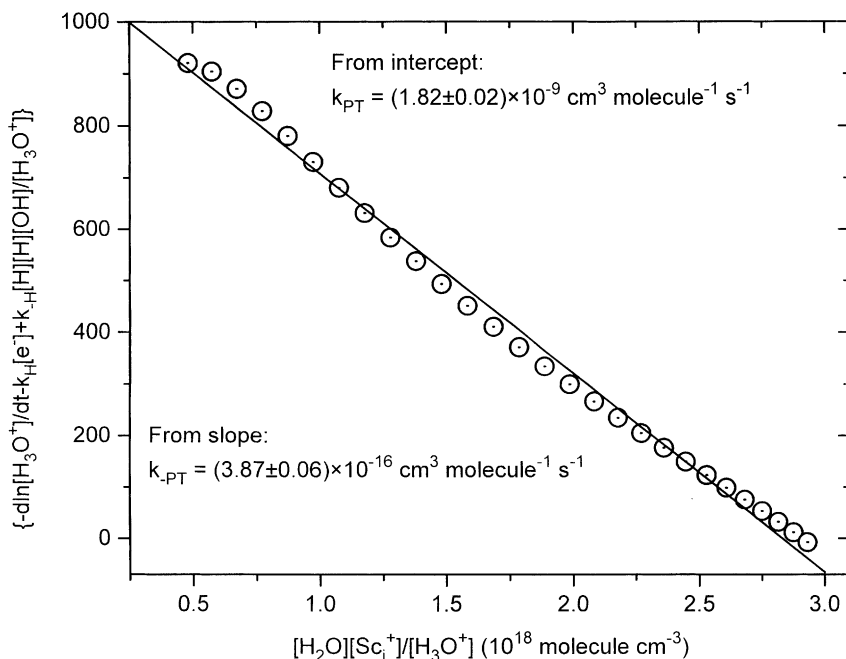


Fig. 6. Sample plot for proton transfer kinetics in flame 2 doped with 0.14 mol% CH_4 and with the atomizer spraying a 0.02 M solution of ScCl_3 .

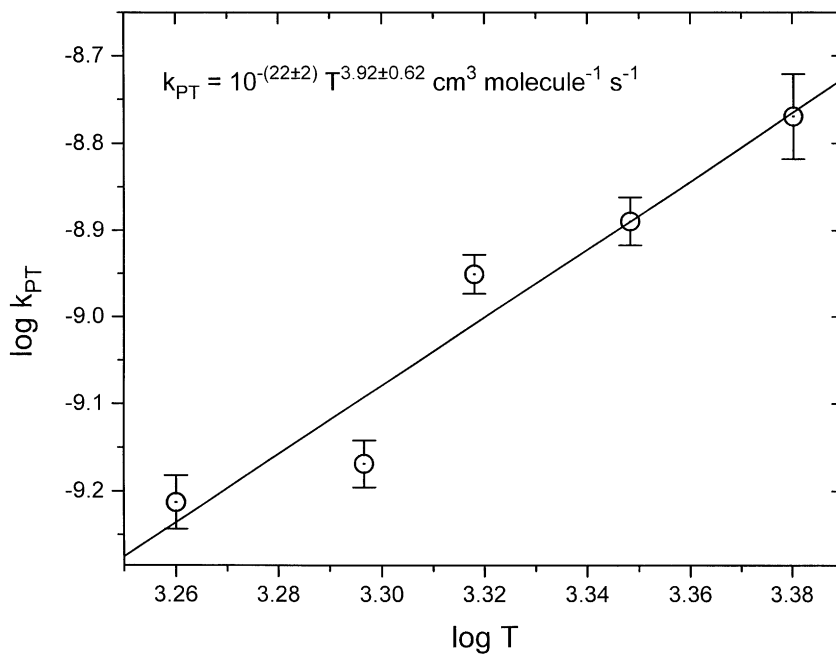


Fig. 7. Temperature dependence of the global rate coefficient for proton transfer by H_3O^+ to scandium neutral species.

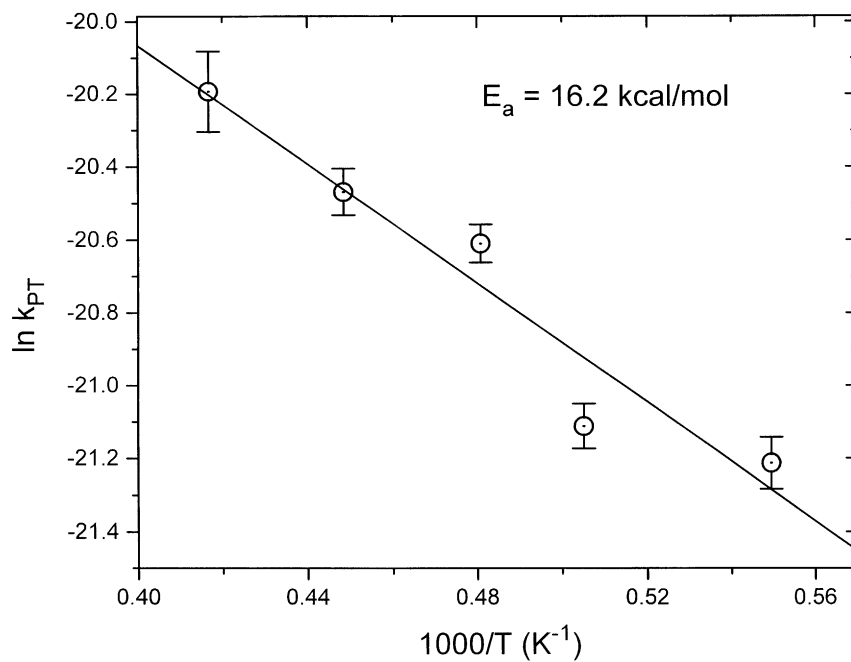


Fig. 8. Determination of the activation energy for the global proton transfer reaction of H_3O^+ to scandium neutral species.

plot given in Fig. 8 generated from the positive temperature dependence in Fig. 7 corresponds to a small activation energy barrier of $16.2 \text{ kcal mol}^{-1}$. At each temperature, the experiments were repeated three to five times and the error bars in Figs. 7 and 8 represent one standard deviation of these measurements.

4.5. Global recombination of scandium ions with electrons

The method of total cation collection as described in Section 3 has been employed to measure profiles of total positive ions along the flame axis [18,19]. The ions are collected on the nozzle plate when it is biased to a voltage of -50 V with respect to the burner. This novel technique has been used previously to measure recombination coefficients for H_3O^+ with e^- , Cl^- , Br^- and I^- at flame temperatures [19]. Accurate results are easily obtained because the mass spectrometric sampling of ions through the nozzle orifice is

avoided. The method has been employed here to measure the recombination of total scandium ions with electrons.

As an example, Fig. 9 presents profiles for flame 5 doped with 0.28 mol% of CH_4 , with and without the atomizer spraying an aqueous 0.1 M ScCl_3 solution. With the atomizer off, essentially all of the flame ions are H_3O^+ ; profile (a) shows the recombination loss of H_3O^+ with electrons e^- . With the atomizer on, scandium ions form in the flame by proton transfer; profile (b) shows the recombination loss of e^- with the total positive ions including all scandium cations and some remaining H_3O^+ . Back at the burner (z or $t = 0$), the two profiles converge showing that other sources of ion production are negligible. The slower decay of profile (b) compared with (a) indicates scandium ions recombine with electrons more slowly than H_3O^+ . The driving force for recombination between cations and electrons is Coulombic which depends on the charge density. In comparison with H_3O^+ , the scandium

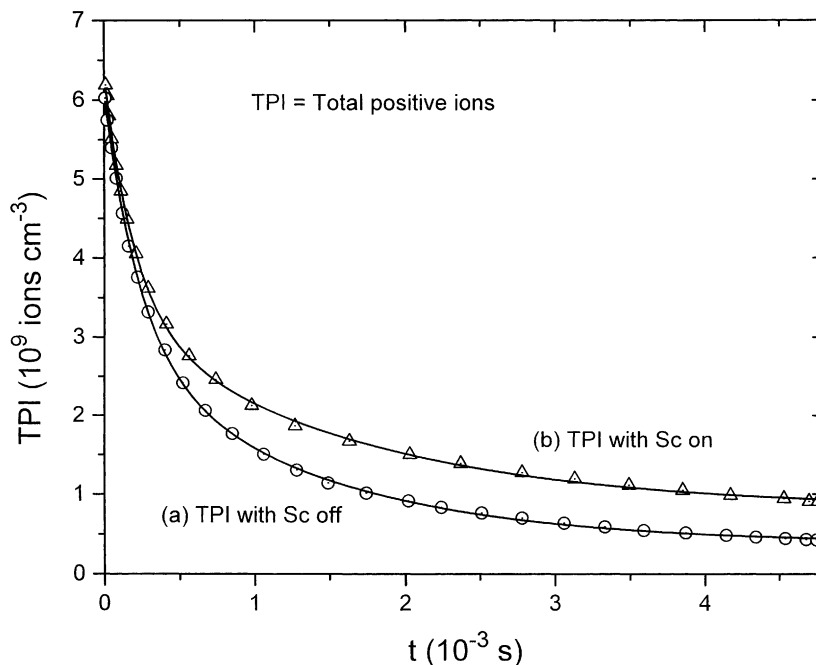


Fig. 9. Total positive ion profiles in flame 5 doped with 0.28 mol% of CH_4 measured by total cation collection at the nozzle plate when -50 V was applied to the nozzle with respect to the burner (a) without scandium, and (b) with the atomizer spraying a 0.1 M solution of ScCl_3 .

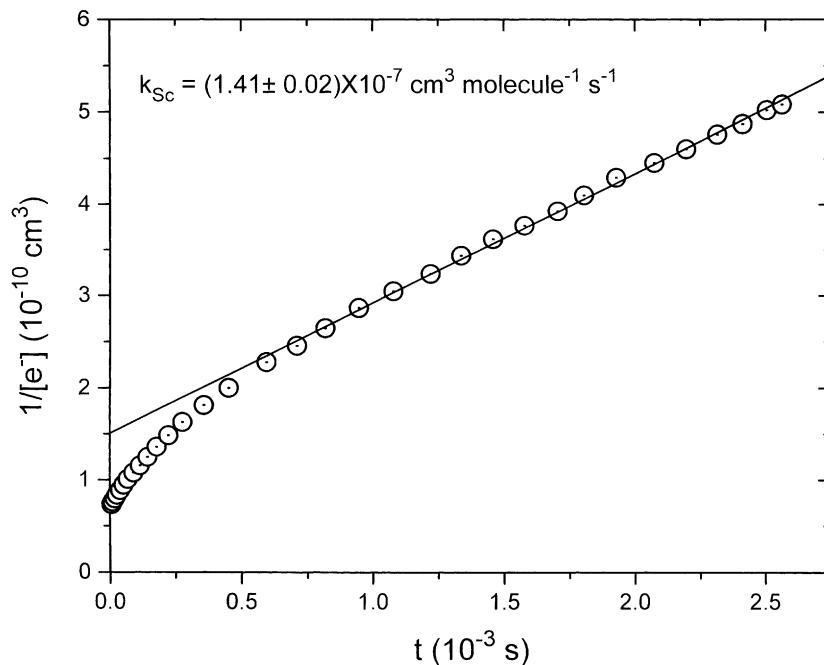
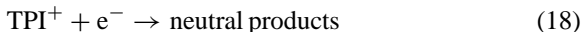


Fig. 10. Sample plot for recombination kinetics of total scandium ions with free electrons in flame 3 doped with 0.17 mol% CH₄ and with the atomizer spraying a 0.1 M solution of ScCl₃.

ions are larger and, consequently, have lower charge densities such that slower recombination might be expected.

The global recombination is a typical second-order reaction with $[TPI] = [e^-]$ because the flame is a quasi-neutral plasma



Plots of $1/[TPI]$ or $1/[e^-]$ vs. time t gave good straight lines from each of which the recombination coefficient was obtained as the slope. Fig. 10 presents a sample plot for flame 3 at 2080 K with the atomizer spraying a 0.1 M ScCl₃ solution. The global recombination coefficient ($1.41 \times 10^{-7} \text{ cm}^3 \text{ molecule}^{-1} \text{ s}^{-1}$ in this example) includes contributions from both scandium ions and H₃O⁺. The contribution from H₃O⁺ can be removed by measuring the ratio of H₃O⁺ to total scandium ions. The latter can be measured separately with the mass spectrometer by setting the mass dial to, say, 50 u with the dc voltage to the quadrupole rods switched off. Measurements made with the higher con-

centration of 0.1 M ScCl₃ solution rather than 0.02 M showed that H₃O⁺ amounted to only a few percent of the total positive ions. Essentially then, the global recombination coefficient obtained from Fig. 9 corresponds to the recombination coefficient for total scandium ions with electrons.

The combined measurements for the global recombination of scandium ions with electrons in five flames are shown as a logarithmic plot in Fig. 11. At each temperature, the experiments were repeated 8–10 times and the error bars represent one standard deviation of these measurements. A straight line through the data yields an overall recombination coefficient given by $k_{sc} = (3.72 \pm 0.22) \times 10^{-4} T^{-1.03 \pm 0.26} \text{ cm}^3 \text{ molecule}^{-1} \text{ s}^{-1}$ with a negative temperature dependence. The value is $1.48 \times 10^{-7} \text{ cm}^3 \text{ molecule}^{-1} \text{ s}^{-1}$ at a representative temperature of 2000 K. Compared with the H₃O⁺/e⁻ recombination coefficient of $(1.32 \pm 0.04) \times 10^{-2} T^{-1.37 \pm 0.05} \text{ cm}^3 \text{ molecule}^{-1} \text{ s}^{-1}$ (which gives 3.96×10^{-7} at 2000 K) [19], k_{sc} is smaller, indicative of slower recombi-

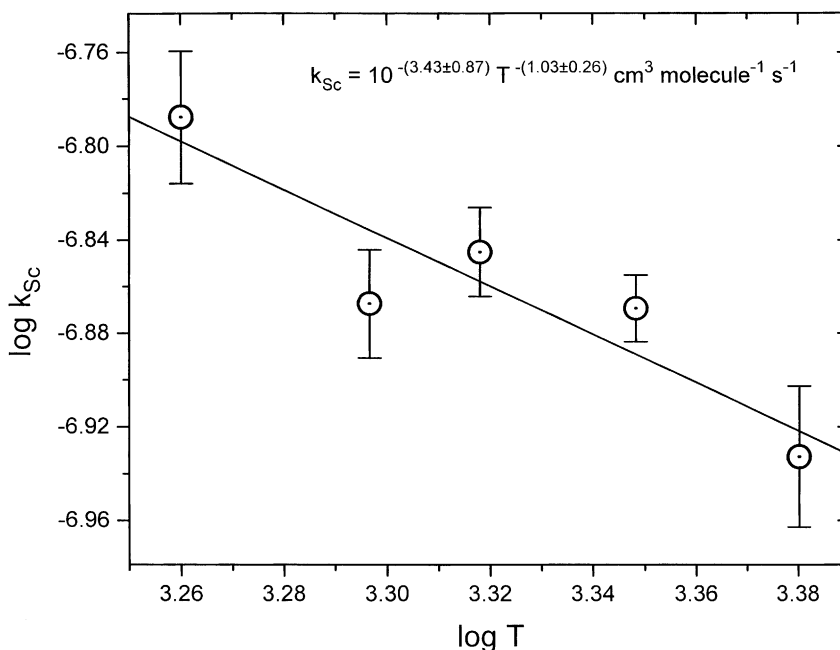


Fig. 11. Temperature dependence of the global recombination coefficient for scandium ions with free electrons.

nation, but has the same negative temperature dependence. From Fig. 2, it is fair to say that that k_{Sc} represents the recombination of electrons primarily with $Sc(OH)_2^+$, and with ScO^+ to a smaller extent.

5. Summary and conclusions

The ionization of scandium was investigated in five fuel-rich $H_2-O_2-N_2$ flames at temperatures in the range 1820–2400 K. The relative concentrations of the scandium neutrals and ions in the five flames were calculated using theoretical thermodynamic data from our previous studies [10]. The calculations indicate the overwhelming predominance of $Sc(OH)_3$ and $OScOH$ out of 11 scandium neutrals, and of $Sc(OH)_2^+$ and ScO^+ out of 20 scandium ions in all five flames. This is in excellent agreement with our experimental observations that the ions are members of the oxide ion series $ScO^+ \cdot nH_2O$ ($n = 0-3$). Experimentally, hydrate ions form mainly due to the cooling which occurs when the flame gas is sampled through the

nozzle into the mass spectrometer. Hydrate ions are further emphasized when the nozzle orifice diameter is decreased or the flame temperature decreases.

The theoretical thermodynamic data were also employed to investigate various possible ionization mechanisms for scandium species in flames. Thermodynamic calculations show that the chemi-ionization of atomic Sc with O is the only exothermic reaction to produce scandium ions in pure $H_2-O_2-N_2$ flames, but it occurs only during a narrow time interval in the flame reaction zone; other chemi-ionization and also thermal (collisional) ionization reactions are too endothermic to make any measurable contribution. CI by proton transfer is an important ionization source for the scandium system in flames if H_3O^+ is present, as shown by the addition of a hydrocarbon such as CH_4 .

With the addition of 0.415 mL s^{-1} of CH_4 (0.14–0.28 mol% for flames 2–5, respectively), rate coefficients k_{PT} for the global proton transfer reaction to scandium neutrals were measured at five flame temperatures. The reaction has a positive temperature

dependence given by $k_{PT} = (9.58 \pm 0.76) \times 10^{-23} T^{3.92 \pm 0.62} \text{ cm}^3 \text{ molecule}^{-1} \text{ s}^{-1}$. This abnormal behavior appears to arise because the global reaction may involve many primary and secondary steps. Consistent with the positive temperature dependence, a small activation energy barrier of $16.2 \text{ kcal mol}^{-1}$ was obtained from an Arrhenius plot.

The recombination of scandium ions with electrons was measured by an accurate novel technique involving total cation collection at the nozzle plate when a negative bias is applied to the nozzle with respect to the burner. Because of the lower charge density on scandium ions, their recombination with electrons is slower than that of H_3O^+ . Similar to $\text{H}_3\text{O}^+/\text{e}^-$, the recombination coefficients for scandium ions exhibit a negative temperature dependence given by $k_{Sc} = (3.72 \pm 0.22) \times 10^{-4} T^{-1.03 \pm 0.26} \text{ cm}^3 \text{ molecule}^{-1} \text{ s}^{-1}$.

The important reactions and mechanisms considered here for Sc are believed to be applicable also to the other group 3 metals Y and La with one significant difference. Thermal (collisional) ionization, although negligible for Sc, will play an additional minor role for Y [6], and a considerably greater one in the case of La [7].

Acknowledgements

Support of this work by the Natural Sciences and Engineering Research Council (NSERC) of Canada is gratefully acknowledged.

References

- [1] J.M. Goodings, Q. Tran, N.S. Karellas, *Can. J. Chem.* 66 (1988) 2219.
- [2] P.M. Patterson, J.M. Goodings, *Int. J. Mass Spectrom. Ion Processes* 148 (1995) 55.
- [3] P.M. Patterson, J.M. Goodings, *Int. J. Mass Spectrom. Ion Processes* 152 (1996) 43.
- [4] J.M. Goodings, C.S. Hassanali, P.M. Patterson, C. Chow, *Int. J. Mass Spectrom. Ion Processes* 132 (1994) 83.
- [5] C.C.Y. Chow, J.M. Goodings, *Can. J. Chem.* 73 (1995) 2263.
- [6] Q.F. Chen, J.M. Goodings, *Int. J. Mass Spectrom.* 176 (1998) 1.
- [7] Q.F. Chen, J.M. Goodings, *Int. J. Mass Spectrom.* 188 (1999) 213.
- [8] J. Guo, J.M. Goodings, *J. Mol. Struct. (Theochem.)* 549 (2001) 261.
- [9] J. Guo, J.M. Goodings, *J. Mol. Struct. (Theochem.)* 571 (2001) 171.
- [10] J. Guo, J.M. Goodings, *Int. J. Mass Spectrom.* 214 (2002) 339.
- [11] M.W. Chase Jr., C.A. Davies, J.R. Downey Jr., D.J. Frurip, R.A. McDonald, A.N. Syverud, *JANAF Thermochemical Tables*, 3rd Edition, *J. Phys. Chem. Ref. Data* 14 (Suppl. 1) (1985).
- [12] A.N. Hayhurst, D.B. Kittelson, *Proc. R. Soc. London, Ser. A* 338 (1974) 155.
- [13] C.J. Butler, A.N. Hayhurst, *J. Chem. Soc., Faraday Trans.* 92 (1996) 707.
- [14] J.M. Goodings, S.M. Graham, W.J. Megaw, *J. Aerosol Sci.* 14 (1983) 679.
- [15] A.N. Hayhurst, D.B. Kittelson, N.R. Telford, *Combust. Flame* 28 (1977) 123.
- [16] A.N. Hayhurst, D.B. Kittelson, *Combust. Flame* 28 (1977) 137.
- [17] N.A. Burdett, A.N. Hayhurst, *Combust. Flame* 34 (1979) 119.
- [18] J.M. Goodings, J. Guo, A.N. Hayhurst, S.G. Taylor, *Int. J. Mass Spectrom.* 206 (2001) 137.
- [19] J. Guo, J.M. Goodings, *Chem. Phys. Lett.* 329 (2000) 393.
- [20] A.N. Hayhurst, D.B. Kittelson, *Proc. R. Soc. London, Ser. A* 338 (1974) 175.
- [21] A.N. Hayhurst, N.R. Telford, *J. Chem. Soc., Faraday Trans.* 1 71 (1975) 1352.
- [22] S.D.T. Axford, A.N. Hayhurst, *J. Chem. Soc., Faraday Trans.* 91 (1995) 827.
- [23] J.A. Green, T.M. Sugden, *Ninth Symposium (International) on Combustion*, Academic Press, New York, 1963, p. 607.
- [24] E.P. Hunter, S.G. Lias, Proton Affinity, NIST Chemistry WebBook, NIST Standard Reference Database Number 69, March 1998 Release (<http://webbook.nist.gov/chemistry/paser.html>).
- [25] S.D.T. Axford, A.N. Hayhurst, *J. Chem. Soc., Faraday Trans.* 91 (1995) 827.